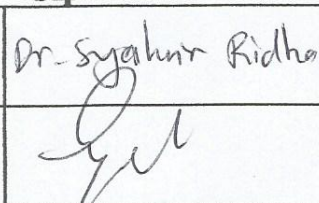
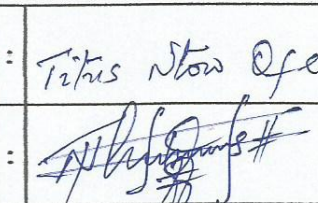


AMENDMENTS CONFIRMATION FORM

Student's Name	:	MURUC NAZMIN BINTI ZULKARNAIN
Student ID	:	13690
Title of the Project	:	MICRO GEOPOLYMER CEMENT WITH ENHANCED PHYSICAL PROPERTIES FOR WELL CEMENTING.

This is to certify that I (supervisor/examiner) have examined the dissertation, and that any and all revisions required by the examining committee have been made. The student is allowed to submit the hardbound.

Supervisor		Internal Examiner			
Name	:	Dr. Syahrir Ridha	Name	:	Titus Nwan Ofei
Signature	:		Signature	:	
Official Stamp	:	Dr Syahrir Ridha Lecturer, Petroleum Engineering Universiti Teknologi PETRONAS	Official Stamp	:	Petroleum Engineering Department Universiti Teknologi PETRONAS Bandar Seri Iskandar, 31750 Tronoh Perak Darul Ridzuan, Malaysia

Micro Geopolymer Cement with Enhanced Physical Properties for Well Cementing

by

Nurul Nazmin binti Zulkarnain

13690

Dissertation submitted in partial fulfilment of
the requirements for the
Bachelor of Engineering (Hons)
(Petroleum Engineering)

MAY 2014

Universiti Teknologi PETRONAS

Bandar Seri Iskandar

31750 Tronoh

Perak Darul Ridzuan

CERTIFICATION OF APPROVAL

Micro Geopolymer Cement with Enhanced Physical Properties for Well Cementing

by

Nurul Nazmin binti Zulkarnain

13690

A project dissertation submitted to the
Petroleum Engineering Programme
Universiti Teknologi PETRONAS
In partial fulfilment of the requirement for the
BACHELOR OF ENGINEERING (Hons)
(PETROLEUM)

Approved by,

(Dr. Syahrir Ridha)

UNIVERSITI TEKNOLOGI PETRONAS

TRONOH, PERAK

May 2014

CERTIFICATION OF ORIGINALITY

This is to certify that I am responsible for the work submitted in this project, that the original work is my own except as specified in the references and acknowledgements, and that the original work contained herein have not been undertaken or done by unspecified sources or persons.

NURUL NAZMIN BINTI ZULKARNAIN

ABSTRACT

Ordinary Portland Cement (OPC) has been used widely in oil well industry. However, OPC creates high permeability between cement particles when exposes to HPHT environment inside the wellbore and also releases large amount of carbon dioxide (CO_2) during manufacturing process. Previous research has been conducted to substitute OPC with geopolymer based cement such as fly ash. Geopolymer cement successfully reduces emission of CO_2 to five to ten times less than OPC but still resulted in the same permeability trend as OPC. This project introduced micro silica in geopolymer cement to study its effect on the permeability problem in OPC and geopolymer cement. Four samples are developed with the percentage of micro silica range from 0% to 60%. The performance of developed samples are compared with Class G Cement (OPC) in term of permeability at HPHT (4000psi and 120 °C) environment for three curing durations; 24 hours, 72 hours and 120 hours and fluid loss at LPLT environment (500psi and 70 °C). Rheology and density test are compared at standard room conditions. The test results show the permeability of cement increase when increase the percentage of micro silica and curing duration. For static fluid loss test, increase in micro silica reduced the volume of filtrate. Two rheological model are observed from the samples; Power Law and Bingham Plastic Model. At standard room condition, the viscosity of cement slurry increased and density of samples decreased when increase the micro silica. Overall, Sample A, B and C can replace OPC up to 4000psi and 120°C condition while all samples have better performance than OPC in term of fluid loss up to 500psi and 70°C, rheology and density environment and standard room condition.

ACKNOWLEDGEMENT

First and foremost, I would like to thank Allah S.T.W. for giving me the opportunity to complete my final year project; Micro Geopolymer Cement with Enhanced Physical Properties for Well Cementing.

This project would not successfully completed without the help of many people and here I would like to express my sincere appreciation to Dr. Syahrir Ridha, Lecturer of Petroleum and Geosciences Faculty for his valuable guidance and advice as my final year project supervisor. My special recognition I bid to Technologist in Petroleum Engineering Laboratory, Mr. Khairul Nizam and Mr. Jukhairi for their help and guidance in handling Class G Cementing experiment.

Special thanks to my family for their supports and advices and everyone that helping and sharing me their knowledge. Thank you.

TABLE OF CONTENTS

CERTIFICATION	i
ABSTRACT	iii
ACKNOWLEDGEMENT	iv
LIST OF FIGURES	vi
LIST OF TABLES	viii
LIST OF ABBREVIATIONS	ix
 CHAPTER 1:INTRODUCTION									
1.1	Background of Study	1
1.2	Problem Statement	3
1.3	Objectives	4
1.4	Scope of Study	4
 CHAPTER 2:LITERATURE REVIEW									
2.1	Ordinary Portland Cement	5
2.2	Geopolymer Cement	7
2.3	Experimental Program	10
 CHAPTER 3:METHODOLOGY									
3.1	Research Methodology	12
3.2	Key Milestones	26
3.3	Project Timelines	27
 CHAPTER 4:RESULTS									
4.1	Permeability Test	28
4.2	Static Fluid Loss Test	33
4.3	Rheology Test	34
4.4	Density Test	39
 CHAPTER 5: CONCLUSIONS & RECOMMENDATIONS									
5.1	Conclusions	42
5.2	Recommendations	43
REFERENCES	44

LIST OF FIGURES

Figure 1.	Cement is pumped between drill string and annulus	2
Figure 2.	Potential gas migration along a well	3
Figure 3.	Geopolymerisation process	8
Figure 4.	Cement Mixer	14
Figure 5.	Fly Ash	14
Figure 6.	Class G Cement	14
Figure 7.	Micro silica	14
Figure 8.	Sodium silicate	14
Figure 9.	Sodium hydroxide pellet	14
Figure 10.	Curing chamber	16
Figure 11.	Greased curing molds	16
Figure 12.	Cement is stirred with stirring rod	16
Figure 13:	Curing molds are tied using thread	16
Figure 14.	Molds are inserted into pressure vessel	16
Figure 15:	Cylinder plug is threaded into pressure vessel	17
Figure 16.	Thermocouple is inserted into pressure vessel	17
Figure 17.	Oil cylinder	17
Figure 18.	Cement samples that have been cured	17
Figure 19.	Cured cement sample surrounded by other cement (bottom view)	18
Figure 20.	Cured cement sample is surrounded by other cement (top view)	18
Figure 21.	Remain in Class G Cement sample after coring process	18
Figure 22.	Cement sample after coring and trimming process	18
Figure 23.	Poroperm	19
Figure 24.	SRATE Microscope	19
Figure 25.	Static Fluid Test	21
Figure 26.	Greased cylinder cell	21
Figure 27.	O- ring	21
Figure 28.	Filter paper	21
Figure 29.	Grooved cap	21
Figure 30.	Top valve installed on grooved cap	21
Figure 31.	Thermocouple inserted through the hole on the cell	22

Figure 32.	Measuring cylinder below the bottom valve	22
Figure 33.	Pressurized mud density balance	24
Figure 34.	Viscometer	24
Figure 35.	Key milestone for this project	24
Figure 36.	Permeability for all samples cured for 24 hours at 4000psi and 120°C	26
Figure 37.	Permeability for all samples cured for 72 hours at 4000psi and 120°C	27
Figure 38.	Permeability for all samples cured for 120 hours at 4000psi and 120°C	27
Figure 39.	Permeability for all samples in 24, 72 and 120 hours curing duration	28
Figure 40.	Permeability variation with inlet pressure at confining pressure of 12MPa	29
Figure 41.	Sample A (24 hours)	30
Figure 42.	Sample D (24 hours)	30
Figure 43.	Sample A (72 hours)	30
Figure 44.	Sample D (72 hours)	30
Figure 45.	Sample A (120 hours)	30
Figure 46.	Sample D (120 hours)	30
Figure 47.	Volume of filtrate for Cement G, Sample A, B, C and D	31
Figure 48.	Linear plot for shear rate vs. shear stress for all samples	33
Figure 49.	Logarithmic plot of shear rate versus shear stress for all samples	34
Figure 42.	Apparent viscosity for Cement G, Sample A and Sample B	35
Figure 51.	Plastic viscosity for Sample C and Sample D	36
Figure 52.	Yield Stress for Sample C and Sample D	37
Figure 53.	Graph of density for Class G Cement, Sample A, B, C and D	38

LIST OF TABLES

Table 1.	Different classes of oil well cement: Class A until Class G	1
Table 2.	The composition of cement and it's weight percentages.	5
Table 3.	Cement Additives	6
Table 4.	Composition of each samples based on percentage	12
Table 5.	Mass of Class G Cement, fly ash, micro silica and alkaline solution for every mix	12
Table 6.	Composition of fly ash Class F	12
Table 7.	Project Timelines	25
Table 8.	k and n values for Cement G, Sample A and B	36
Table 9.	Plastic viscosity and yield stress for Sample C and D	38
Table 10.	Density for Class G Cement, Sample A, B, C and D.	40

LIST OF ABBREVIATIONS

API	=	American Petroleum Institute
ASTM	=	American Society for Testing and Materials
CaCO ₃	=	Calcium Carbonate
CaO·2SiO ₂ ·4H ₂ O	=	Calcium Silicate Hydrate
Ca ₂ SiO ₄	=	Dicalcium Silicate
Ca ₃ SiO ₅	=	Tricalcium Silicate
Ca (OH) ₂	=	Calcium Hydroxide
HPHT	=	High Pressure High Temperature
H ₂ O	=	Water
LPLT	=	Low Pressure Low Temperature
Na ₂ SiO ₃	=	Sodium Silicate
NaOH	=	Sodium Hydroxide
Na ₂ O	=	Sodium Oxide
r/min	=	Revolution per Minute
SiO ₂	=	Silicon Dioxide

CHAPTER 1

INTRODUCTION

1.1 BACKGROUND

Cement is defined as a binder agent for construction materials. In an oil well, cement is used to provide zonal isolation between casing and formation, prevents the occurrence of a blowout, protects the casing from shock load while drilling in deeper formation and protects the casing from corrosion. Eventhough petroleum industry had begun in 1859 with the establishment of Drake Well, cement started being used in Lompoc, California in 1903 to shut off the down hole water just above the oil sand [1]. Cement used in construction has different properties compared to cement used for oil well cementing. Table 1 shows the type of cement used for oil well cementing with different properties and depths.

Table 1. Different classes of oil well cement: Class A until Class G [1]

Cement Classes	Descriptions
Class A	Depth: 0ft to 6000ft
Class B	Depth: 0ft to 6000ft. Moderate to high sulfate resistance.
Class C	Depth: 0ft to 6000ft High early strength.
Class D	Depth: 6000ft to 10000ft. Moderate to high pressure high temperature.
Class E	Depth: 10000ft to 14000ft. HPHT well.
Class F	Depth: 10000ft to 16000ft. HPHT well. Moderate to high sulfate resistant.
Class G&H	Depth: 0ft to 8000ft Wide range of temperature and pressure. Can be used with retarder or accelerator. Act as basic cement.

In construction, cement often exposes to ambient temperature and pressure while in the wellbore, cement exposes to high pressure and high temperature conditions which will change the properties of cement. In oil well cementing, cement will be pumped

from the surface to the target location in the well through the drill string. Then, it will fill in the space between the annulus and the casing as shown in the Figure 1. Two types of cementing process involve in oil well operation:

1. Primary cementing: To full fill the objective of cementing such as providing zonal isolation between casing and formation.
2. Remedial cementing: Repair the primary cementing or treat the conditions arising after wellbore has been constructed.

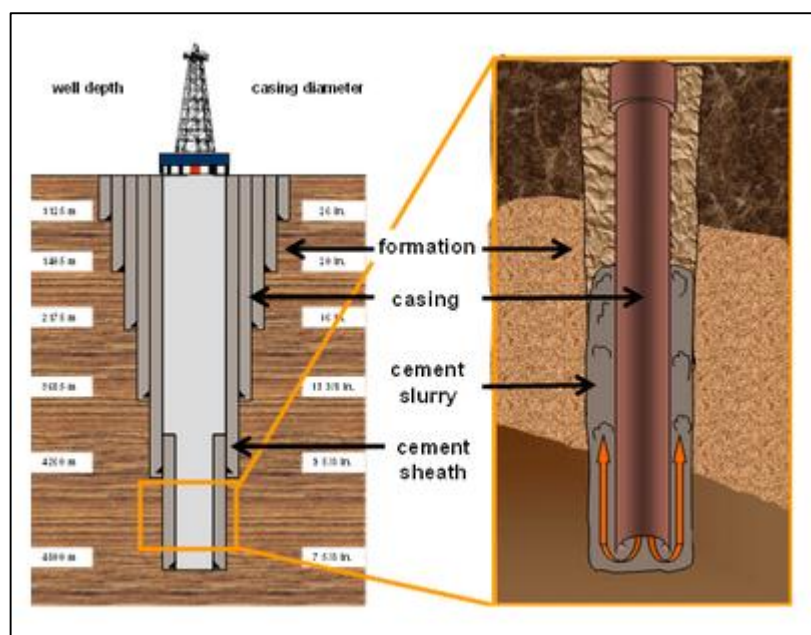


Figure 1. Cement is pumped between drill string and annulus

1.2 PROBLEM STATEMENT

- i. Ordinary Portland Cement (OPC) and geopolymer based cement create high permeability when exposed to high temperature in down hole condition. Cement with high permeability allow the migration of gas between cement particles (Figure 2) which can reduce cement integrity and may lead to blowout.
- ii. Manufacturing of OPC is estimated to release about 3.24 billion tons of CO₂ each year and expected to grow in the range of 3680 million tons to 4380 tons in 2050 [8], [9].

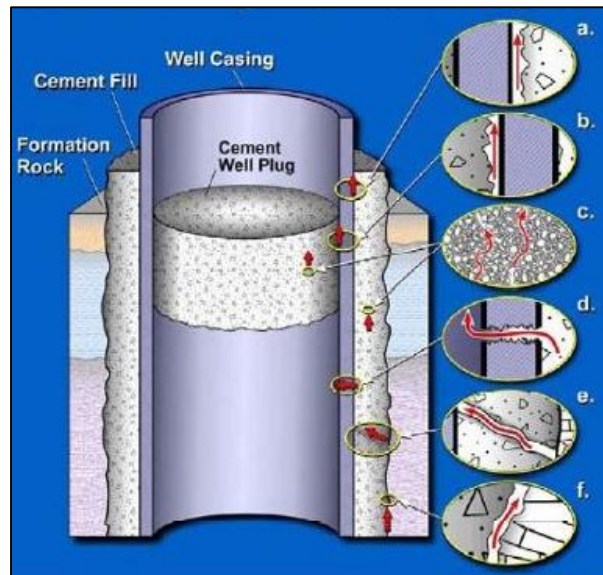


Figure 2. Potential gas migration along a well [21]

1.3 OBJECTIVES

- i. To develop micro green cement and examining its physical properties; permeability, fluid loss, rheology and density.
- ii. To examine the physical properties of micro green cement.
- iii. To compare the permeability performance of micro green cement with Class G Cement (standard oil well cement) at 4000psi and 120 °C for three curing conditions; 24hours, 72hours and 120hours, evaluate fluid loss performance at 500psi and 70 °C and compare the rheology and density of cement samples at standard room condition.

1.4 SCOPE OF STUDY

Development of micro green cement for oil well cementing from micro silica and fly ash, consisting of study the properties of micro silica and fly ash as micro green cement, conducting researches on the ratio of alkaline activator and molarity of alkaline solution required to develop micro green cement. Physical properties of developed micro green cement will be examined in term of permeability, volume of filtrate, rheology and density test in standard room condition. The physical properties for micro green cement will be compared with Class G Cement.

CHAPTER 2

LITERATURE REVIEW

2.1 ORDINARY PORTLAND CEMENT (OPC)

Portland cement is made up of five major compounds and few minor compounds. The composition of typical Portland cement are listed in Table 2 [30]:

Table 2. The composition of cement and its weight percentages.

Cement Compound	Weight Percentages
Tricalcium Silicate	50%
Dicalcium Silicate	25%
Tricalcium Aluminate	10%
Tetracalcium Aluminoferrite	10%
Gypsum	5%

Compressive strength of Portland cement is developed through hydration; chemical reaction between water and cement compound. Silicate contributes to the strength of cement. Tricalcium silicate plays a major role in early strength development while dicalcium silicate involves in developing the cement strength at later times as the reaction of dicalcium silicate is slower compares to tricalcium silicate. Equations below show the reaction of tricalcium silicate and dicalcium silicate with water and both reactions are exothermic [30].

Tricalcium Silicate + Water → Calcium Silicate Hydrate + Calcium Hydroxide + Heat



Dicalcium Silicate + Water → Calcium Silicate Hydrate + Calcium Hydroxide + Heat



The rheology is developed from reaction of aluminate compound at the beginning of hydration. Aluminate also contributes in developing the early strength of the cement. Rate of hydration can be controlled by adding gypsum to prevent premature hardening of cement. Gypsum will reacts with aluminate and hydroxyl ion to form ettringite.

Ettringite will prevent hydration process by forming needle shaped crystal on the aluminate and creating induction period (slow hydration period) [11].

Some additives as shown in Table 3 can be added to cement slurry to enhance the properties of oil well cement.

Table 3. Cement Additives [11]

Additives	Descriptions
Accelerator	To speed up the early stages of hydration. Applicable in shallow well.
Retarder	Inhibit hydration and slow the setting time of cement. Applicable in deep well.
Extender	Reduce slurry density, thus reduce the hydrostatic pressure during Class G Cementing operation. Extender is used to prevent break down and loss of circulation of weak formation.
Weighting agent	Increase cement density by adding high specific gravity material to the slurry.
Dispersant	Control slurry rheology by reducing viscosity of slurry.
Fluid loss control agent	Use to control loss of water from cement to formation.
Loss circulation agent	Reduce fluid loss from the cement into weak formation.

Oil well cement demands to have rapid gain in strength and neither shrink due to heat, moisture, drying nor dehydration. Early strength development is important in ensuring structural support to casing, hydraulic and mechanical isolation [16]. It can also be set in the presence of sulphate water, be a pump able slurry and produces no lumps, remain fluid until close to setting time, do not produce excessive heat during setting of cement and has low permeability to prevent migration of gas [16].

In down hole, OPC often exposes to failure such as crack due to pressure and temperature changes inside the wellbore [1], [3]. High temperature resulted in loss of silica in cement due to degradation. Inadequate presence of silica will convert calcium silicate hydrate (C-S-H) phase into lime rich α -dicalcium silicate hydrate. α -dicalcium silicate hydrate creates high permeability and strength retrogression in the cement mix [3], [16].

Permeability is the ability of fluid to flow through interconnected porous medium. Low permeability of cement is good for a long term performance of cement while high

permeability may lead gas percolation, result in pressure accumulation behind low portion of the well. It also may cause blowout, bad zonal isolation and production losses [16], [17].

Strength retrogression can be defined as a reduction in cement strength to the point of failure due to exposure of high temperature [19]. Strength reduction also can be affected by other factors. Cyclic pressure load may cause formation fissure to get wider over time and result in material failure [6]. The greater the compressive strength, the more susceptible it is to stress cracking [11]. Other than that, cement also faces the stress from formation pore pressure which can caused cement degradation. Cement degradation also occurs due to geochemical attack such as corrosive agent. [1]. Moreover, cement which have free water or settling tendencies can result in water channel on the top side or at the area of reduce compressive strength and thus good zonal isolation cannot be achieved [12].

2.2 GEOPOLYMER CEMENT

Geopolymer technology involves the converting of byproduct to valuable product. It can be defined as large groups of binder which solidify after the activation of reactive solid (geopolymer raw materials) in high alkaline environment. Geopolymer has been used in numerous application such as fire heat resistant, waste encapsulation, fiber composite, concrete and cement. Geopolymer cement has been developed since 1905 and known as alkaline activator cement [7], [22].

The difference between geopolymer cement and OPC lies in the different of energy uses for activation process. OPC uses high energy to activate the material before reacting with low energy material, such as water during calcination process while, geopolymer use low energy material such as fly ash to react with small amount of high energy solution, for example sodium hydroxide to create the reaction between those materials. Due to low energy required for manufacturing of geopolymer cement, it can be concluded that geopolymer cement releases five to ten times less the amount of carbon dioxide emission compares to OPC [31], [37].

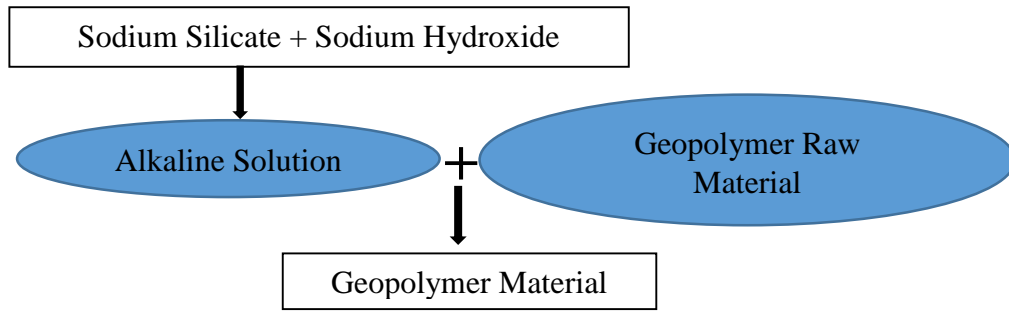


Figure 3. Geopolymerisation process

Figure 3 show the process of geopolymerisation that consists of three steps. First, the dissolution of aluminosilicates in highly alkaline solution. Alkaline solution consist of soluble alkali metal either potassium or sodium base with sodium silicate or potassium silicate. Silicate helps in enhancing the gelation process of geopolymer cement [23], [24]. The solubility of aluminosilicates in the alkaline solution depends on the concentration of the hydroxide solution; increase in the concentration of hydroxide solution will increase the solubility of aluminosilicates.

Next, reorientation of free ions cluster take place after the dissolution process and followed by polycondensation. Polycondensation involves the process of forming aluminosilicates polymer network; three dimensional polymeric chain and ring structure consisting of Si-O-Al-O bonds. In overall, geopolymerisation involves the process of leaching, diffusion, condensation and harden network which occur under atmospheric pressure with temperature below 100 °C [22].

Previous research concluded that geopolymer cement poses high excellent acid resistance as acid tends to prevent alkali from leaching, higher strength, high pump ability and lower shrinkage compared to OPC [3], [5]. It is good for environment with temperature higher than 30 °C as silica and aluminium from raw materials already dissolves in alkaline activator. Increase in down hole temperature will increase the rate of reaction in producing brittle matrix, but possibility of breaking of geopolymer intergranular might occur if temperature goes beyond 100 °C which can lead to strength reduction [3].

2.2.1 Fly Ash

Fly ash is byproduct from coal burning that have cementitious characteristic similar to Portland cement and it rich with silica and alumina [9], [24]. It can be used to substitute limestone up to 40% by weight of cement [2]. Fly ash also known as artificial pozzolan which is defined as siliceous and aluminous material, natural or artificial, process or unprocessed which contains cementitious constituents. It will reacts with calcium hydroxide in the presence of moisture at ordinary temperature to form relatively stable and water insoluble compound possessinClass G Cementitious properties [15].

Fly ash contain heterogeneous mixtures of silicon oxides, aluminium oxides and iron oxides [9]. The types of coal burned and nature of combustion process determine the binding properties of fly ash [8]. Fly ash contributes in increasing the mechanical activation due to increase in the surface area [7]. Applying fly ash as raw material in cement manufacturing can reduces CO₂ emission and high energy required for calcination process [7].

ASTM C618 defined two types of fly ash; Class C and Class F. The difference between Class C and Class F are based on the amount of calcium, silica, alumina and iron content in the ash. Class C contains high calcium, sodium and magnesium which is produced from burning of the low rank coals such as lignite and subbituminous coal while Class F has little calcium, higher silica and iron content which is produced from bituminous coal [25].

2.2.2 Micro Silica

Micro silica is a by-product from the reduction of high – purity quartz with coal. It is produced from silicon and ferrosilicon alloys in electric furnace and was first commercially used in 1969 [38], [39]. Micro silica is categorized as highly effective pozzolanic material due to its extreme fineness and high silica content with 85% to 95% of amorphous SiO₂ [40]. Act as extender, micro silica allows 0.532 gallons of water to be added to the cement slurry per pound of micro silica [38]. Hydrostatic pressure durinClass G Cementing will reduces due to decrease in cement density. Therefore, it is possible to do cementing in low pressure or depleted reservoir pressure.

Induced loss of circulation due to breakdown of weak formation can be prevented too [41].

Plastic viscosity and yield point of cement will increase when micro silica mix with Portland cement. Strong network between micro silica and cement is created due to increasing of slurry gels as the micro silica tends to absorb more water in the solution [40].

With the average size of 0.1 μm , micro silica particles can fill in the pores between cement particles and block the narrow passages of fluid, thus lowering the permeability of cement. Gas percolation through unset cement can be restricted when gas permeability reduced [38]. In addition, micro silica can reduce the fluid loss into the permeable formation through bridging and blocking between the cement particles. Cement permeability and fluid loss can also be improved through uniform dispersion between cement particles and micro silica [41].

High reactivity of micro silica will increase the strength of cement due to increase rate of dehydration. Previous research shows 64% gain in strength in 8 hours and 43% gain in strength when 2% By Weight of Cement (BWOC) of micro silica is added to the cement class H [38].

High temperature in wellbore condition can caused cement retrogression. Portland cement will transform crystalline phases into alpha silica hydrate, a weak and porous compound when the cement is exposed to temperature higher than 230°F. By adding 35% of micro silica to cement slurry, a strong and impermeable crystalline phase called tobermerite will form. At temperature higher than 150°C, tobermerite will convert into xenotlite with traces of gyrolite. The compressive strength of xenotlite is exceed 5000 psi [38], [42].

2.3 EXPERIMENTAL PROGRAM

In preparing geopolymer cement, two ratios need to be considered; water geopolymer solid (WGS) ratio and alkaline solution to fly ash (AL: FA) ratio. WGS ratio must be equivalent as water cement ratio (WCR) in Portland cement in order to compare

geopolymer cement with OPC. It can be achieved by having the same mass or by having the same volume of cementitious materials as OPC in WCR [29]. WGS and WCR affect the workability of cement itself. By reducing these ratios, cement workability can be improved but it will reduce its early strength.

In WGS ratio, the water component is the total mass of water used in making alkaline solution plus any extra water added to the mixture. Geopolymer solid is the sum of the mass of sodium silica solid, sodium hydroxide solid and fly ash. For alkaline solution to fly ash ratio, alkaline is mass of alkaline used in the mixture, for example the total mass of sodium silicate solution and sodium hydroxide solution. Fly ash is the mass of fly ash alone [27].

CHAPTER 3

METHODOLOGY

3.1 RESEARCH METHODOLOGY

- i. Preparation of cement slurry
- ii. Laboratory test of cement slurries
- iii. Tabulations and interpretation of laboratory test result data

3.1.1 Preparation of Cement Slurries

Preparation of cement slurries are based on API RP 10-A Section 7. Five samples are prepared (Table 4) from Class G Cement (Figure 5), fly ash (Figure 6) and micro silica (Figure 7). The mass for each material in every mix is presented in Table 5. The composition of Class F fly ash are presented in Table 6. No additive is added in all samples. The propeller type mixing device is used to prepare cement slurry (Figure 4).

Table 4. Composition of each samples based on percentage

Samples	Class G Cement	Fly Ash Class F	Micro Silica
Class G Cement	100%	0%	0%
A	0%	100%	0%
B	0%	80%	20%
C	0%	60%	40%
D	0%	40%	60%

Table 5. Mass of Class G Cement, fly ash, micro silica and alkaline solution for every mix in grams

Samples	Class G Cement	Fly Ash Class F	Micro Silica	Sodium Silicate	Sodium Hydroxide	Water
Class G Cement	500	0	0	178.59	71.43	100.15
A	0	500	0			
B	0	400	100			
C	0	300	200			
D	0	200	300			

Table 6. Composition of fly ash Class F

Composition as oxide	Al ₂ O ₃	SiO ₂	Fe ₂ O ₃	K ₂ O	MgO	Na ₂ O	SO ₃	Loss of ignition
Typical values, weight %	23.74	56.70	5.97	1.49	0.73	0.40	0.65	5.06
Composition as oxide	CaO	ZrO ₂	SrO	NiO	CuO	P ₂ O ₅	MnO	ZnO
Typical values, weight %	3.98	0.05	0.04	0.02	0.025	0.048	0.024	0.017

3.1.1.1 Water Cement Ratio and Water Geopolymer Solid Ratio

WCR and WGS ratio = 0.44 according to water cement ratio for Class G Cement. The mass method is used for WGS ratio but due to lesser specific gravity of fly ash and micro silica, the volume of fly ash and micro silica are larger compared to Class G Cement. Alkaline solution to fly ash ratio of 0.5 is chosen based on previous research [24]. To obtain the same ratio for WGS with WCR, 100.15g of water is added in every geopolymer cement samples.

3.1.1.2 Alkaline Solution

Sodium silicate (Figure 8) and sodium hydroxide (Figure 9) are used as alkaline activators and the ratio of sodium silicate to sodium hydroxide is 2.5 which is believed to give an effective reaction between these two solutions [23], [24], [27], [33]. Sodium silicate solution of Grade A53 which contains Na₂O = 14.7%, SiO₂ = 29.4% and water = 55.9% is used in this experiment. 361grams of sodium hydroxide in pellet form with 99% purity is dissolved in 1000 grams of distilled water to produce 12M sodium hydroxide solution [23], [24]. Both alkaline solutions are made constant for all samples.

3.1.1.3 Mixing Procedures [34]

- i. All materials are weighted according to Table 5.
- ii. The mixer is turned on. Mixing container is filled with wet materials and placed on the mixer motor.
- iii. Mix 1 button with rotation of 4000r/min +/- 200 r/min is pressed for 15seconds. In this moment, all the dry materials is poured into the mixing container.
- iv. Mix 2 button is pushed after the 15seconds. The rate of rotation is increase from 4000r/min +/- 200r/min to 12000r/min +/-500r/min for 35seconds.
- v. Cement slurry is ready.

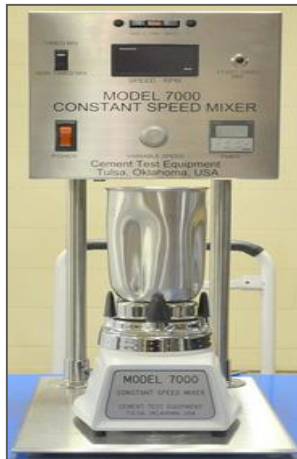


Figure 4. Mixing device



Figure 5. Class G Cement



Figure 6. Fly Ash



Figure 7. Micro silica



Figure 8. Sodium silicate



Figure 9. Sodium hydroxide pellet

3.1.2 Laboratories Test of Cement Slurries

3.1.2.1 Permeability

Permeability is defined as the ability of fluid to flow within the cement particles when subjected to differential pressure under the helium flow. Permeability mathematically equated by Darcy law.

$$k = \frac{(2000 \times OP \times Q \times \mu \times L)}{A \times IP^2 - OP^2}$$

Where Q = Flow rate, litre/s

k: Permeability, md

L: Length, cm

A: Cross Sectional Area, cm²

μ: Viscosity, cp

OP: Outlet Pressure, atm

IP: Inlet Pressure, atm

Good cement should provides low permeability to prevent the gas migration between the cement particles. In this project, permeability of gas for all samples are tested using Poroperm (Figure 23) according to API 10B-2, Section 11.

Before proceeding to permeability test, the samples need to be cured to simulate the wellbore condition (4000psi and 120°C) in curing chamber (Figure 10) for three different durations and cored to have the size of Poreporm holder.

Preparation of Cured Cement Samples

- i. Curing molds are greased on the inner surface before assemble (Figure 11).
- ii. Prepared cement slurry is poured into the assembled molds. The cement is poured in three layers. In every layer, cement slurry is paddled using the stirring rod to destroy the bubbles in the cement slurry (Figure 12). Then, all the molds are clamped using the threaded rod (Figure 13).
- iii. Curing chamber is switched on.
- iv. The molds are lowered into the pressure vessel (Figure 14). The cylinder plug thread is lubricated using grease. The cylinder plug thread is threaded into the cylinder (Figure 15). Then, the set screws on top of the cylinder thread are tightened using spanner three different torques (15, 30 and 40 ft-lbs).
- v. A thermocouple is inserted through the hole on top of cylinder plug and is tied loosely (Figure 16).
- vi. The air supply is opened and the flow of oil into pressure vessel is monitored through oil cylinder (Figure 17). The thermocouple is tightened with a spanner when the oil expelled from the thermocouple.
- vii. The pump is on and off until the pressure reached 4000 psi.
- viii. The temperature is set in the program list. In this project, 120 °C is chosen as the temperature.
- ix. The heater is on and followed by the timer.
- x. Then, *auto* and *run* button is pressed to start the operation. The durations of the operation are varied in every experiment: 24hours, 72 hours and 120 hours. Figure 18 shows the cured cement samples after 24hours.



Figure 10. Curing chamber



Figure 11. Greased curing molds

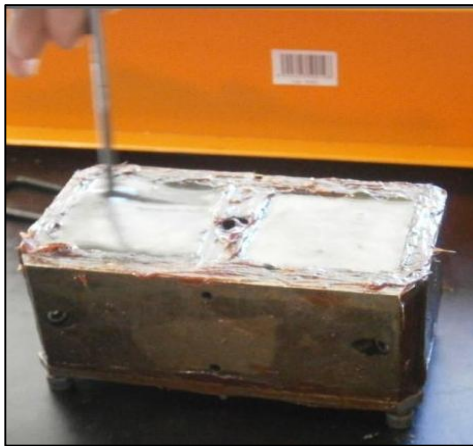


Figure 12. Cement is stirred with stirring rod



Figure 13. Curing molds are tied using thread



Figure 14. Molds are inserted into pressure vessel



Figure 15. Cylinder plug is threaded into pressure vessel



Figure 16. Thermocouple is inserted into pressure vessel



Figure 17. Oil cylinder



Figure 18. Cement samples that have been cured

Procedures of Core Cutting

The cured cement samples need to be cored using core cutting saw to be in cylinder shape. Before coring, the cured cement sample are surrounded by other cement which act as a holder as shown in Figure 19 and Figure 20.

- i. The cement sample is placed in the core cutting saw holder.
- ii. The switch is on.
- iii. The water supply is opened which act as lubricant during the coring process.
- iv. The rotating cutter is pulled down slowly to cut the cement sample and get a cylinder shape for cured cement (Figure 21) (diameter of cylinder = 1.5inch). The remaininClass G Cement holder after coring process is shown in Figure 22.

Procedures for Core Trimming

Cored sample is trimmed with core trimming saw machine to get at least 1.0 inches in length.

- i. Cement sample is placed in the core trimming holder.
- ii. The switch is on and water supply is automatically on which act as lubricant during trimming operation.
- iii. The trimming process is started by pushing the cement holder through the saw.



Figure 19. Bottom view of cement holder



Figure 20. Top view of cement holder



Figure 21. Cement sample after coring and trimming process



Figure 22. The remaininClass G Cement after coring process is done

Procedures for Permeability Test using Poroperm (Figure 23)

- i. The core sample with a standard size (1.0 inch in length and 1.5 inches in diameter) is placed in the core holder.

- ii. The confining pressure with 400psi and the injection pressure is 100psi are applied for all samples.
- iii. All the sample inputs (diameter, length and weight) are inserted into the computer programme.
- iv. The experiment started by clicking on the *start* button on the computer screen.
- v. The permeability of the sample is then recorded and tabulated.

Microstructure View

The microstructure view for all samples are done using SRATE microscope with 10x resolution (Figure 24).

Procedures for Microstructure View:

- i. The specimen is cut into 1 to 3cm and placed on the specimen table.
- ii. LED light is turned on and the microstructure of cement can be seen from binocular head.



Figure 23. Poroperm

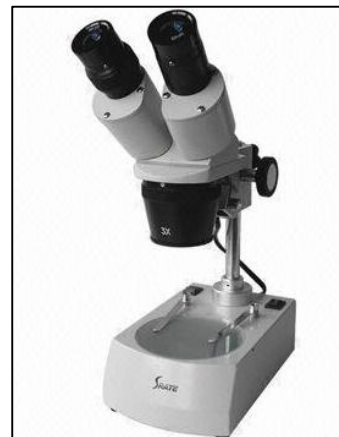


Figure 24. SRATE Microscope

3.1.2.2 Static Fluid Loss Test [58]

Static fluid loss test is done to measure the slurry dehydration after the completion of cementing process. The volume of filtrate at certain differential pressure is recorded. The test is conducted according to API 10B-2, Section 10 using static fluid loss tester (Figure 25) at low pressure low temperature condition (LPLT) at 500psi and 70°C.

Static Fluid Test Procedures [58]:

- i. The fluid-loss cell is greased on the inner part. The cell is dried and cleaned before grease (Figure 26).
- ii. Prepared cement slurry is then poured into the cell until the fill line.
- iii. Next, O-ring is inserted in the cell, next to the fill line (Figure 27).
- iv. A 325 filter mesh (Figure 28) is placed next to the O-ring and again another O-ring is placed after the filter mesh.
- v. A grooved cap is installed after the filter mesh and tighten using an Allen key (Figure 29).
- vi. The valve is installed above the grooved cap and is tighten using a spanner (Figure 30). The valve is closed. This valve acted as bottom valve by changing the position to the bottom.
- vii. The cell is then placed into heating jacket (on fluid loss tester). Another valve and valve adapter are installed, tighten and closed at the top before connecting to the pressure source.
- viii. A thermocouple is inserted through the hole at the top of the cell (Figure 31).
- ix. The switch is on and the temperature increment is observed at the thermocouple. The desired temperature is 158 °F (70°C).
- x. When desired temperature is reached, the pressure at the pressure source (nitrogen) is set to 500 psi. Then, the top valve is opened to let the pressure flow through the cell.
- xi. Measuring cylinder is placed below the bottom valve and the bottom valve is opened (Figure 32).
- xii. The volume of filtrate is then recorded in each five minutes.



Figure 25. Static Fluid Test [58]



Figure 26. Greased cylinder cell



Figure 27. O- ring [58]

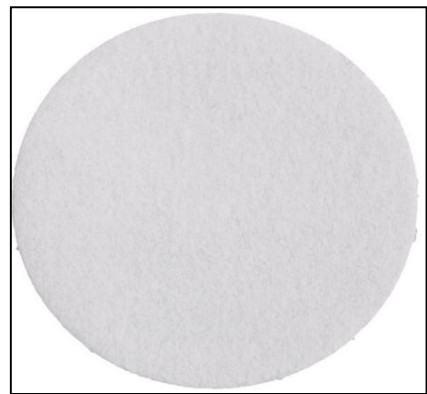


Figure 28. Filter paper



Figure 29. Grooved cap [58]



Figure 30. Top valve installed on grooved cap [58]



Figure 31. Thermocouple inserted through the hole on the cell [58]



Figure 32. Measuring cylinder below the bottom valve [58]

3.1.2.3 Rheological Measurement

Rheology measurement aim to observe the friction pressure and flow regime of the slurry and thus determine the pump ability of the cement to the target location. The viscometer is run with different shear rate, then the shear stress value can be read from calibrated scale. The fluid that has been placed between outer cylinder and inner cylinder caused the viscous drag. This viscous drag produced torque at the boob which transmits precision to the calibrated scale. The test is done according to API Spec 10B-12.4 at standard pressure and temperature using viscometer (Figure 34). There are two types of rheological model for cement slurry: Bingham Plastic Model and Power Law Model. Bingham Plastic Model consist of PV and YP. Plastic viscosity (PV) is defined as resistance of fluid to flow, with lower PV provides better hole cleaning and lower equivalent circulating density at the bottom. Yield point (YP) is the ability of the cement slurry to lift the cutting out of annulus where high YP of cement is desirable [32]. PV and YP can be calculated based on this formula.

$$PV = \theta_{600} - \theta_{300}, \quad YP = \theta_{300} - PV$$

In Power Law Model, apparent viscosity will decrease as the shear rate increase and can be calculate using this formula where k is consistency index, γ is shear rate and n is power law exponent [35].

$$\mu_a = k\gamma^{n-1}$$

Rheology Measurement Procedure [35]:

- i. The rotor slot and groove are aligned with the lock pin in the main shaft socket. Then, the rotor is pushed upward and turned into counterclockwise to lock it.
- ii. The cement was poured into the viscometer cup to the fill line.
- iii. The stage is raised so that the rotor is fully immersed to the proper immersion depth.
- iv. The cement slurry was stirred with the lowest rate, 5.11s^{-1} and the reading is taken after the shear stress values constant at the scale. Step 4 is repeated with other rates value, 10.2s^{-1} , 170s^{-1} , 340s^{-1} , 511s^{-1} and 1020s^{-1} .
- v. All readings are recorded for further interpretation.

3.1.2.4 Slurry Density Test

Density test is done to determine hydrostatic head of cement slurry according to the procedure specified in API Spec 10B-6. The test used pressurized mud balance (Figure 33) and conducted at standard pressure and temperature. Slurry is poured into fixed volume sample cup and the entrained air is compressed with lid to produce more accurate result.

Density Test Procedure [35]:

- i. The sample cup is filled with cement slurry to a level slightly below the upper edge of the cup [$6\text{ mm} \pm 0, 5\text{ mm}$ (1/4 in)].
- ii. Lid is placed on the cup with the check valve in the down (open) position. The lid is pushed downward until the excess slurry expel through check valve.
- iii. The sample cup is then pressurized by maintaining downward force on the pump cylinder housing in order to hold the check valve down (open) and at the same time the piston rod is forced inward.
- iv. The exterior of the cup is then rinse and wiped. Then sliding weight is moved right and left until the beam is balanced which can be seen from the centered attached bubble between two scribed marks.
- v. The density of cement slurry is read from calibrated scales on the arrow side of the sliding weight.



Figure 33. Pressurized mud density balance



Figure 34. Viscometer

3.1.3 Tabulation and Interpretation of Result

All the result will be recorded, tabulated, interpreted as in Chapter 4 (Result and Discussion).

3.2 KEY MILESTONES

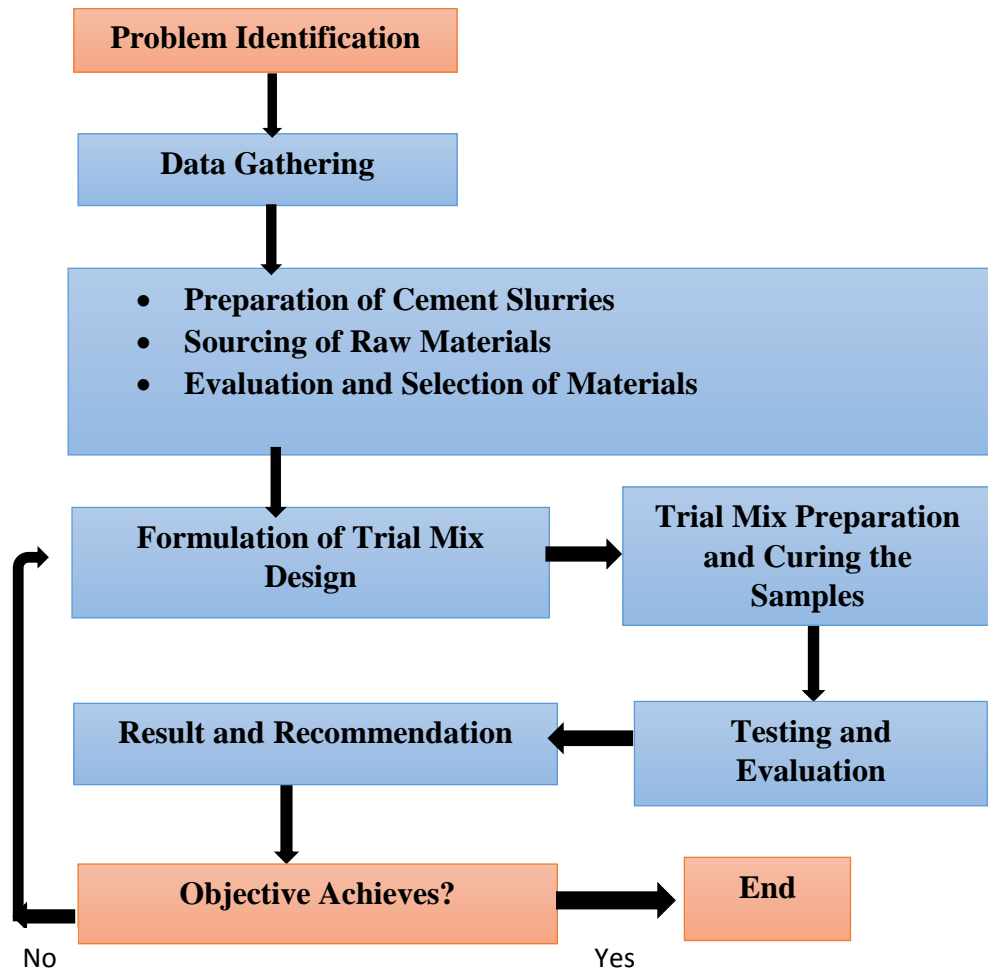


Figure 35. Key milestone for this project

3.3 PROJECT TIMELINES

Table 7. Project Timelines

TASK/ WEEK	2	3	4	5	6	7	8	9	10	11	12	13	14	15	16	17	18	19	20	21	22	23	24	25	26	27	28	
Preliminary Research Work	■	■	■	■	■	■	■	■																				
Preparation of Cement Slurries									■	■	■	■	■	■	■	■	■	■	■	■	■							
Laboratory Test									■	■	■	■	■	■	■	■	■	■	■	■	■							
Result Interpretation																■	■	■	■	■	■	■	■	■				
Report Writing								○													○							

- 1 Proposal Defence
- 2 Interim Report (17th April)
- 3 Progress Report (9th July)
- 4 Pre Sedex (23rd July)
- 5 Final draft Project Report and Technical Paper (13th August)
- 6 VIVA

CHAPTER 4

RESULT AND DISCUSSION

Class G Cement is oil cement recommended by API. The performance for Sample A, B, C and D are compared with Class G Cement for four test conducted.

4.1 PERMEABILITY TEST

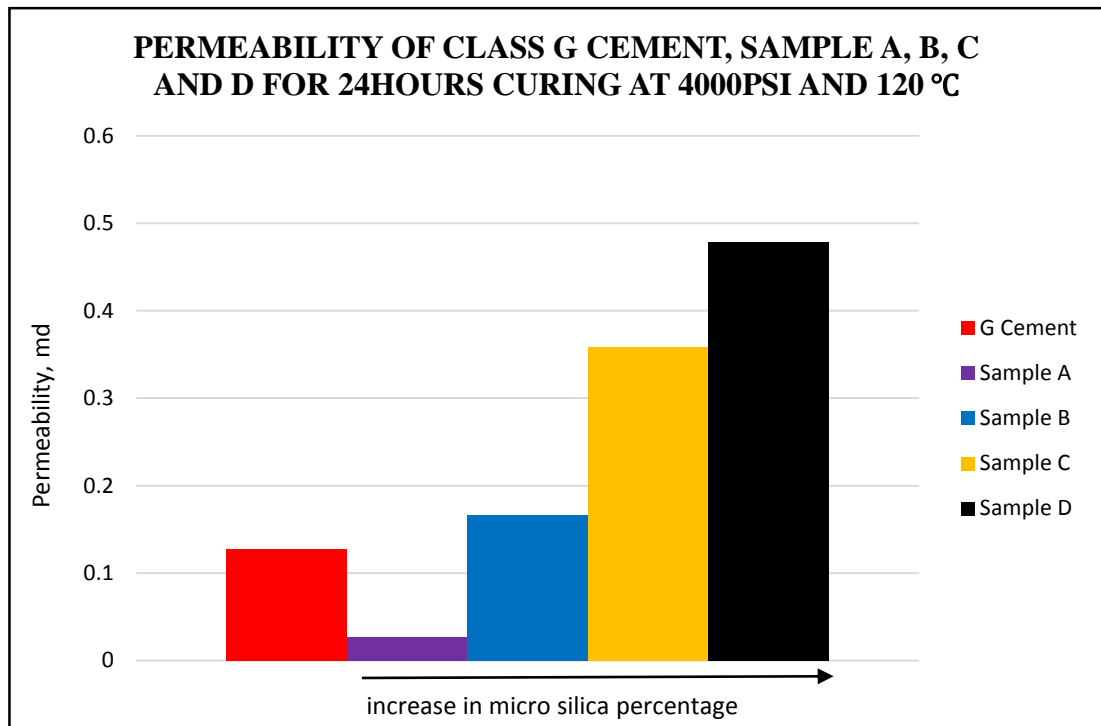


Figure 36. Graph of permeability for all sample cured for 24 hours at 4000psi and 120 °C

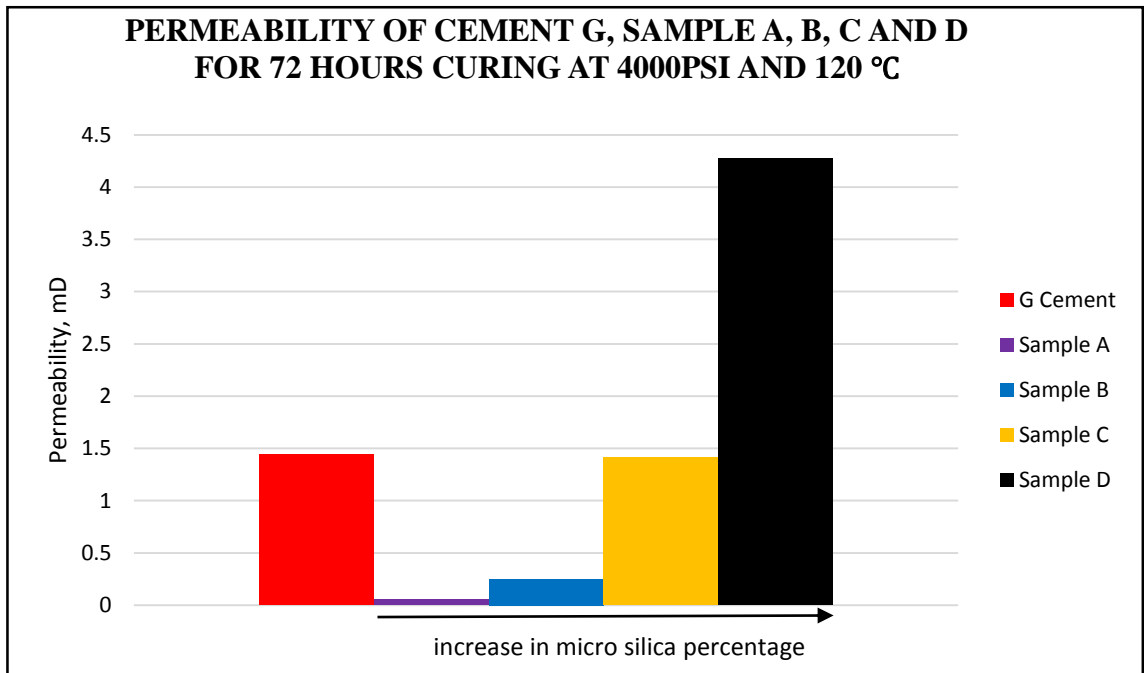


Figure 37. Graph of permeability for all samples cured for 72 hours at 4000psi and 120 °C

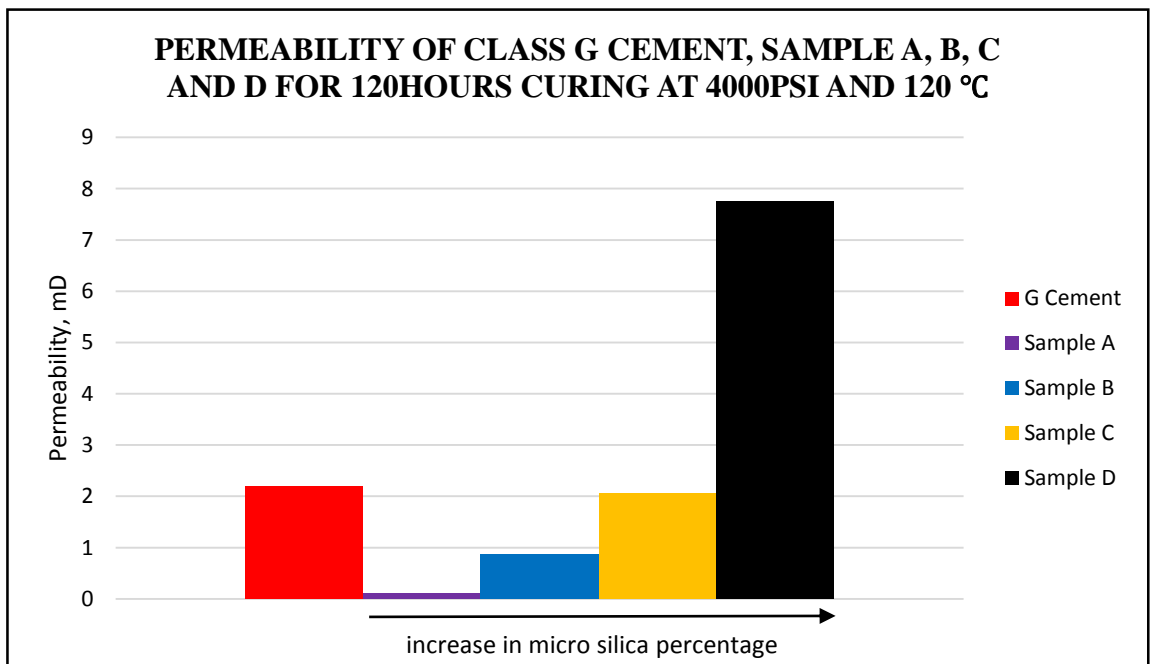


Figure 38. Graph of permeability for all samples cured for 120 hours at 4000psi and 120 °C

As mentioned in the literature review, the permeability of cement samples should decrease when micro silica increase. However, the result for Sample A, B, C and D are not as expected. All cement samples show increase in the permeability when increase in micro silica percentage.

For 24 hours curing duration (Figure 36), Sample D show the highest permeability which is 276% higher than Class G Cement while only Sample A (100% fly ash) has lower permeability compared to Class G Cement with 78.7% differences. For 72 hours and 120 hours curing duration (Figure 37 and Figure 38) respectively, only Sample D has higher permeability than Class G Cement while the permeability of Sample A, B and C are below Class G Cement.

For 72 hours, the permeability for Sample D is 196 % higher while for 120 hours the permeability for Sample D is 255% higher than Class G Cement. The permeability of developed cements also increase as the curing duration increase as shown in Figure 39.

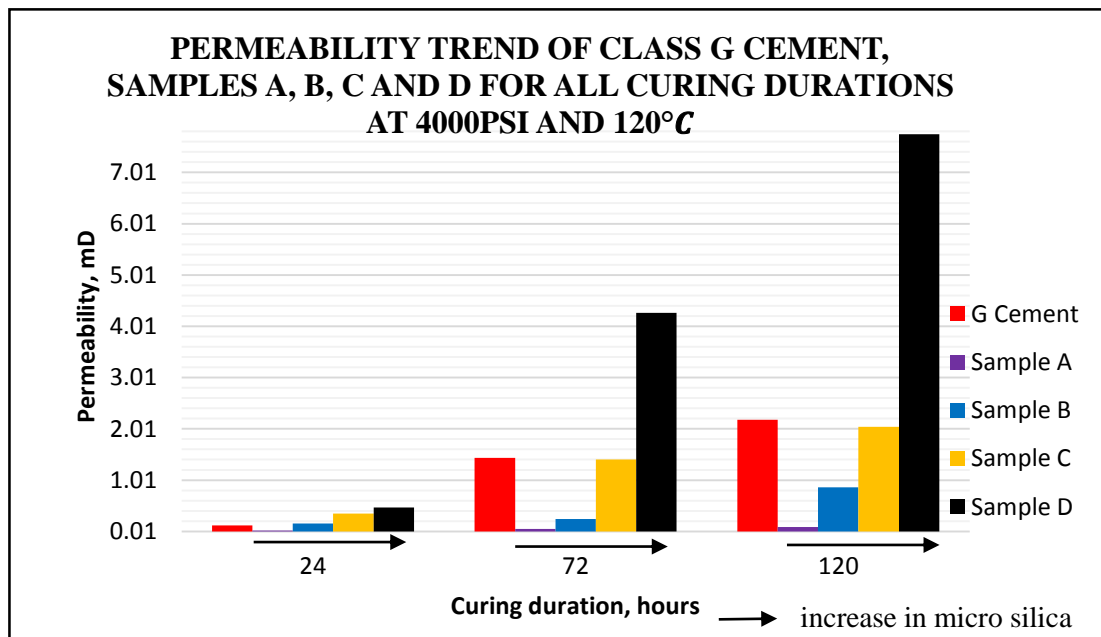


Figure 39. Permeability of Class G Cement, Sample A, B, C and D for all curing duration

As mentioned in literature review, micro silica help in lowering the permeability of cement but the permeability showed by Figures 36, 37, 38 and 39 are contradicting with the literature review. The permeability increase when micro silica increase. Increase in permeability in Sample A, B, C and D are expected due to weakening of the pore structure and pore connectivity of the cement samples when it is exposed to high temperature.

120 °C is stated as high temperature for common well. At lower temperature, particles react slowly thus left large amount of unreacted particles. The geopolymerisation will continue with these unreacted particles, thus reduce pore space and pore connectivity over time and thus decrease the permeability of cement sample. Nevertheless, high temperature resulted in rapid hardening in geopolymer cement, but poor quality geopolymer matrix (highly heterogeneous pore structure) [56].

Micro silica tends to absorb more water compared to Ordinary Portland Cement due to high specific surface area. Increase in the percentage of micro silica will increase the water demand. However, higher temperature increases the rate of moisture loss from the cement samples resulted in inadequate water. Inadequate water increase the potential of crack (permeability will increase too) as water is needed for crack free geopolymer [56].

Research by Nasvi et al. [56] has the same trend of result with this experiment. Figure 40 presents the graph of permeability versus inlet pressure for 24 hours curing. Eventhough permeability decrease as inlet pressure increase but for the same inlet pressure, it is observed the permeability of cement increase as the temperature increase from 23 °C to 70°C. From the permeability trend it can be concluded if Nasvi. et al. [56] use temperature more than 70°C, the expected permeability for 120 °C might be higher than 0.1 mD and will be similar to permeability obtained from this experiment. Nasvi et al. also indicated, the permeability of Class G Cement also increases when increasing the curing duration [56].

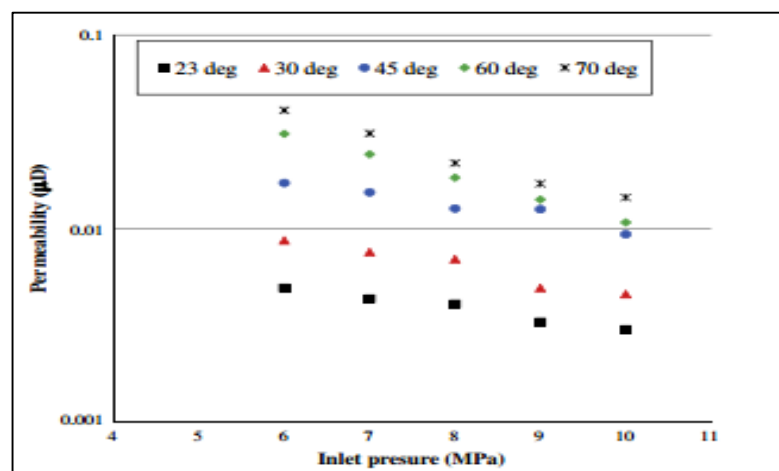


Figure 40. Permeability variation with inlet pressure at confining pressure of 12MPa [56]

Microscopic View

The structure of all samples are viewed under microscope with 10x resolution and the results are in Figures 41, 42,43, 44, 45 and 46.



Figure 41. Sample A (24 hours)



Figure 42. Sample D (24 hours)



Figure 43. Sample A (72 hours)



Figure 44. Sample D (72 hours)

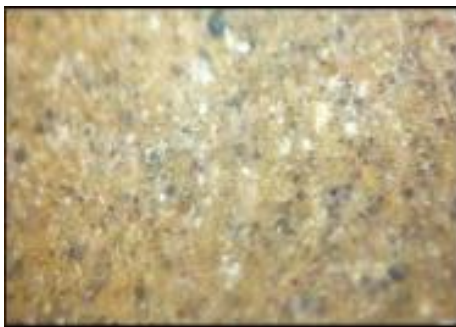


Figure 45. Sample A (120 hours)

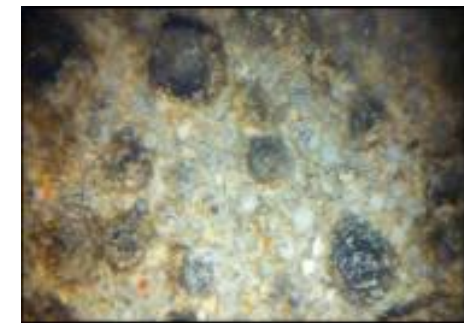


Figure 46. Sample D (120 hours)

Figures above present the microstructure of Sample A and Sample D when exposed to high temperature and high pressure for 24 hours, 72 hours, and 120 hours. Sample A which contain 0% of micro silica seems to have same microstructure and no obvious difference can be detected on the sample from all different curing duration. However for Sample D, increase in black hole (expected as degrade micro silica) when increase in curing duration are observed. These figures (Figures 42, 44 and 46) proved the result

presented by graph in Figure 39 increase in curing duration caused the degradation micro silica to be higher.

4.2 STATIC FLUID LOSS TEST

Static fluid loss test is done to observe the effectiveness of developinClass G Cement in retaining it water phase or to lose it as a filtrate to the formation when subjected to differential pressure across the permeable medium. Inadequate water caused cement dehydration and reduce the pump ability of cement to the target location. 50ml/30 min is an ideal fluid loss according to API standard [49].

When cement reached its target place, the cement filter cake may form against the formation wall. High permeability of cement filter cake cause high fluid loss from the cement to the formation. The cement pore pressure will decrease and gas influx may be induced into the cement.

In this project, all samples have been tested with low pressure, low temperature condition with 500psi and 70 °C for 30 minutes using static fluid loss tester in accordance with API standard. The volume of filtrate is taken in every 5minutes. The result for all samples are presented in the Figure 47.

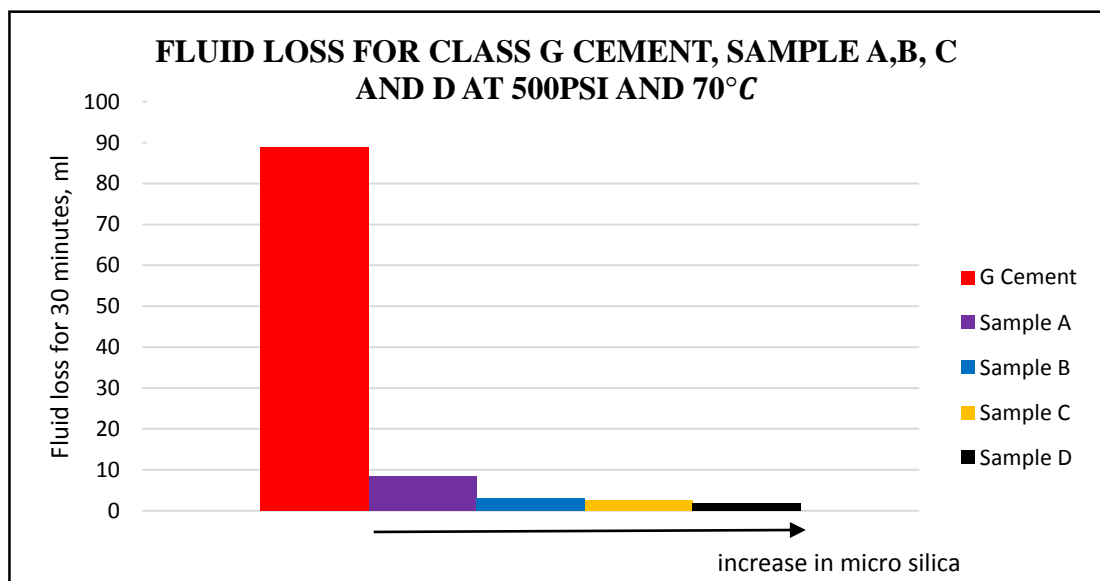


Figure 47. Volume of filtrate for 30 minutes for Cement G, Sample A, B, C and D

From the result, Class G Cement shows the highest fluid loss while sample D which contain 40% of fly ash and 60% of micro silica has lowest fluid loss. However, Sample A, B, C, and D show ideal API Standard for fluid loss with volume of filtrate are below 50ml in 30 minutes.

Increase in the percentage of micro silica improves cement fluid loss and bleeding. The small size of micro silica which is less than 0.5 micrometer act as micro filler between cement and fly ash particles, hence block the passages of fluid between these particles and in cement filter cake thus reduce the volume of fluid loss.

Based on previous research, tiny particle of fly ash and micro silica will react with excess calcium oxide and calcium hydroxide during early hydration to form additional cementitious material of tricalcium silicate and fill in the void space between the cement particles [28].

In addition, higher percentage of micro silica is expected to increase water demand of cement and reduce the possibility of fluid loss to occur [51], [52], and [53]. Increase the percentage of micro silica will prevent the bleeding inside the cement due to the large surface area of micro silica compared to fly ash and Class G Cement. Most free water is used in wetting of the large surface area of the micro silica and hence the free water left in the mix water that may bleed decrease [54]. Bleeding is the settling of solid particle inside the cement and water phase which tends to push to the top of the cement. As cement particle settles to the low side, a continuous water channel formed on the upper side, creating a path for gas migration [55].

All these concepts explain why sample D which contain higher percentage of micro silica has lowest filtrate and Class G Cement which has biggest particle size has highest filtrate (exceed the ideal range of fluid loss) [51].

4.3 RHEOLOGY

Rheology measurements are performed at standard condition and scatter plots (Figure 48 and Figure 49) are prepared to determine the rheological data for each sample. For good cementing operation, cement with low viscosity and low yield stress are needed to produce low equivalent circulating density during pumping.

According to Figure 48 and Figure 49, all samples have been categorized into two rheological models; Bingham Plastic Model and Power Law Model and all samples show non Newtonian fluid behavior.

Class G Cement, Sample A and Sample B have demonstrated Power Law Model while Bingham Plastic Model is presented by Sample C and Sample D (Figure 48). A log-log graph of shear stress versus shear rate has been prepared (Figure 49) to support the results from linear plots. Based on API Recommended Practice 10B-2 Section 12, Power law Model resulted in a straight line in the log- log graph as shown by Sample C and Sample D while Bingham Plastic Model produced a curve as presented by Cement G, Sample A and Sample B.

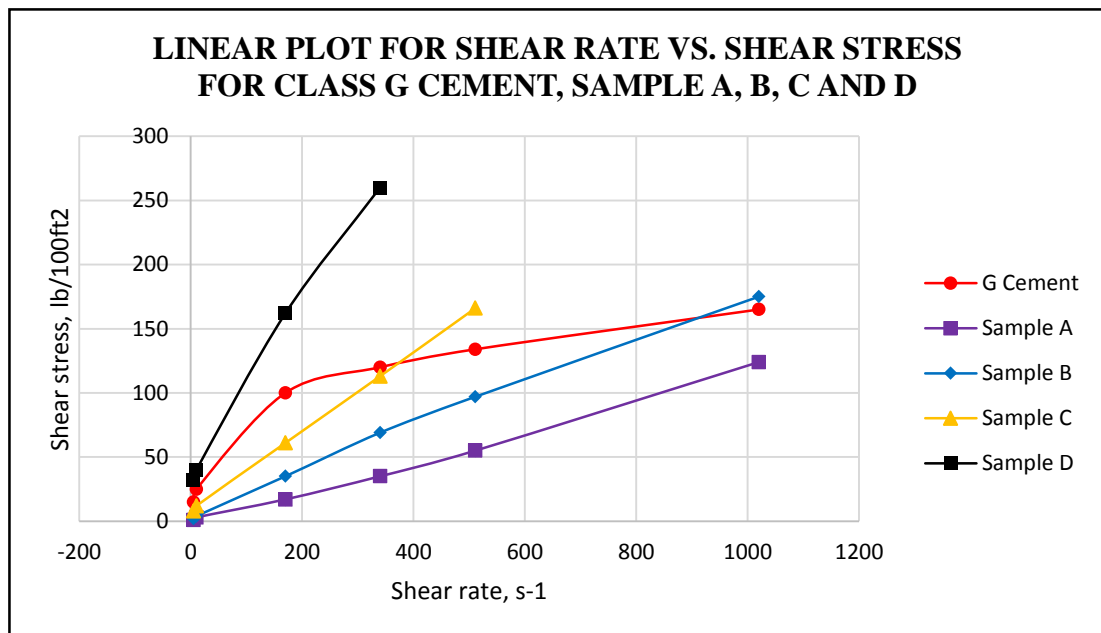


Figure 48. Linear plot for shear rate vs. shear stress for all samples

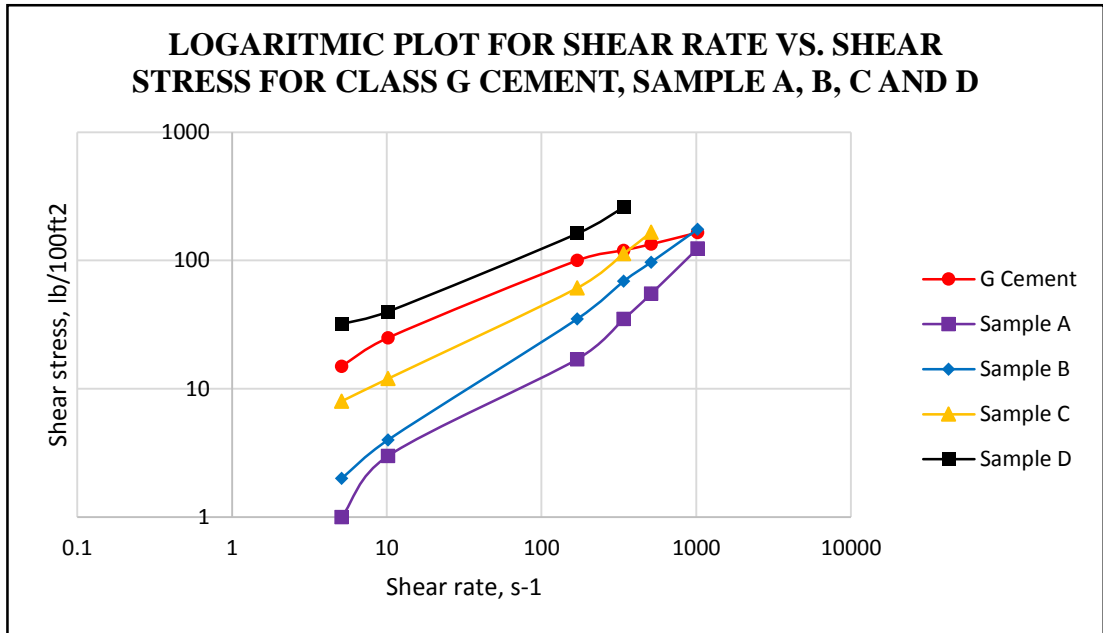


Figure 49. Logarithmic plot of shear rate vs. shear stress for all samples

Comparison on Cement G, Sample A and Sample B for Power Law Model.

The power law model is identified by this formula [35]:

$$\tau = k\gamma^n$$

τ = shear stress, k = consistency, γ = shear rate and n = power law exponent.

Table 8 presented the values for k and n for Cement G, Sample A and Sample B obtained from the equations on linear graph.

Table 8. k and n values for Cement G, Sample A and B

Samples	$k, \text{ lbf. s}^n / \text{ft}^2$	n
Cement G	0.081972	0.4495
Sample A	0.002505	0.8533
Sample B	0.005372	0.831

Consistency index, k measure the viscosity of the fluid, while n measures the degree of deviation of cement slurry from Newtonian behavior [43]. k is proportional to the apparent viscosity of power law fluid as shown by the formula:

$$\mu_a = k\gamma^{n-1}$$

The higher the value of k , the more viscous the fluid. From Figure 50, Sample A and Sample B exhibit desired result. Both samples shows lower apparent viscosity than Class G Cement for every shear rate value. Lower apparent viscosity is preferred in Class G Cementing operation to avoid loss of circulation during placement of cement.

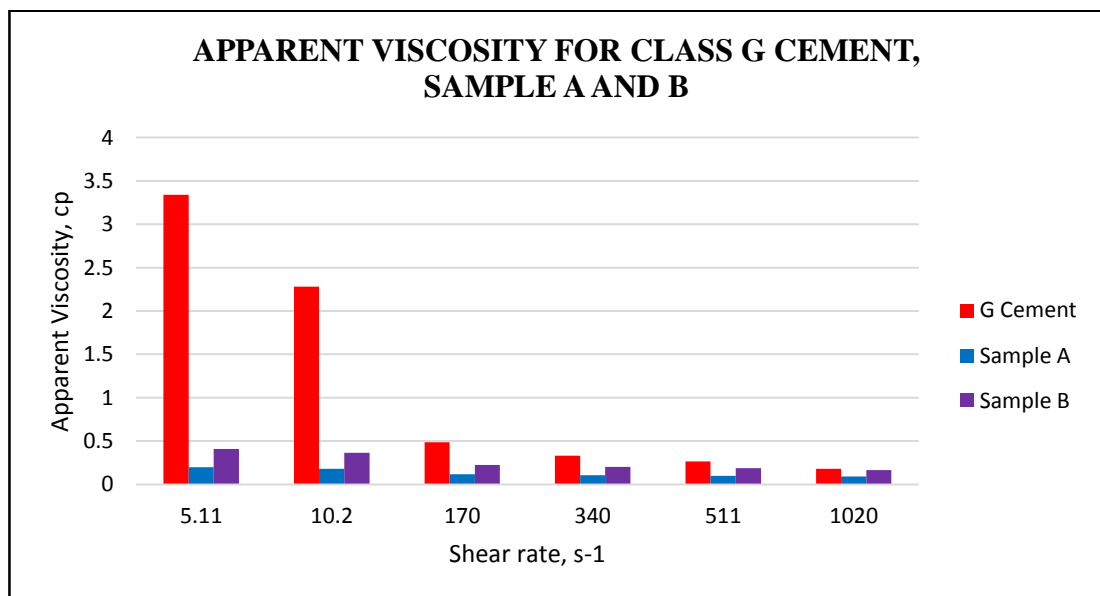


Figure 50. Apparent viscosity for Cement G, Sample A and Sample B.

Increase in the percentage of micro silica in cement sample resulted in high apparent viscosity due to high specific surface of micro silica compared to Cement G and fly ash. Specific surface area for micro silica is 63000 to 150000 ft²/lb, 1400 to 3400 ft²/lb for fly ash and Portland cement has a specific surface area of 1500 to 2000 ft²/lb [47]. Increase in surface area will increase the water requirement. In this experiment, the volume of water to cement or water to geopolymer are made constant for all samples. Therefore, the samples which contains high micro silica experienced

inadequate water and tend to form gels between its particles [41], [45]. High specific surface area also enhances the attractive forces between cement particles, resulted in strong networks for the samples that contain high micro silica [44].

Bingham Plastic Model for Sample C and Sample D

Bingham Plastic Model is presented by this formula:

$$\tau = \mu_p \gamma + \tau_y$$

where τ : shear stress μ_p : plastic viscosity γ : shear rate τ_y : yield stress

$$\text{Plastic viscosity} = \theta_{600} - \theta_{300}$$

$$\text{Yield Point} = \theta_{300} - PV$$

Table 9. Plastic viscosity and yield stress for Sample C and Sample D

Samples	Plastic Viscosity	Yield Stress
	cp	lb/100ft²
Sample C	147.85	8.2048
Sample D	329.08	38.235

As mentioned, the viscosity of cement slurry increase when there is an increase in micro silica and this trend can be observed from Figures 51 and 52.

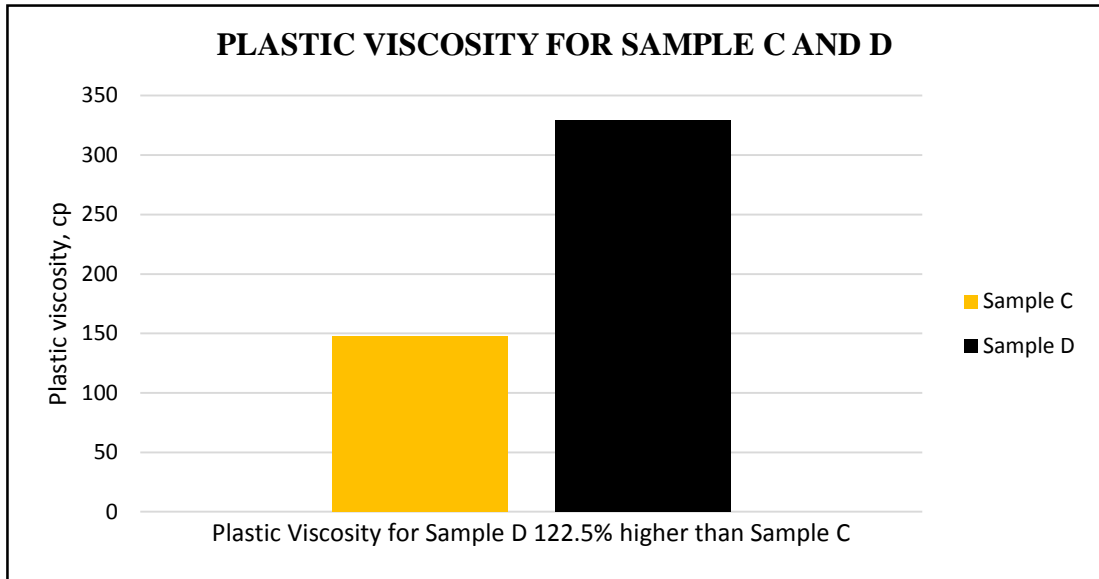


Figure 51. Plastic viscosity for Sample C and Sample D

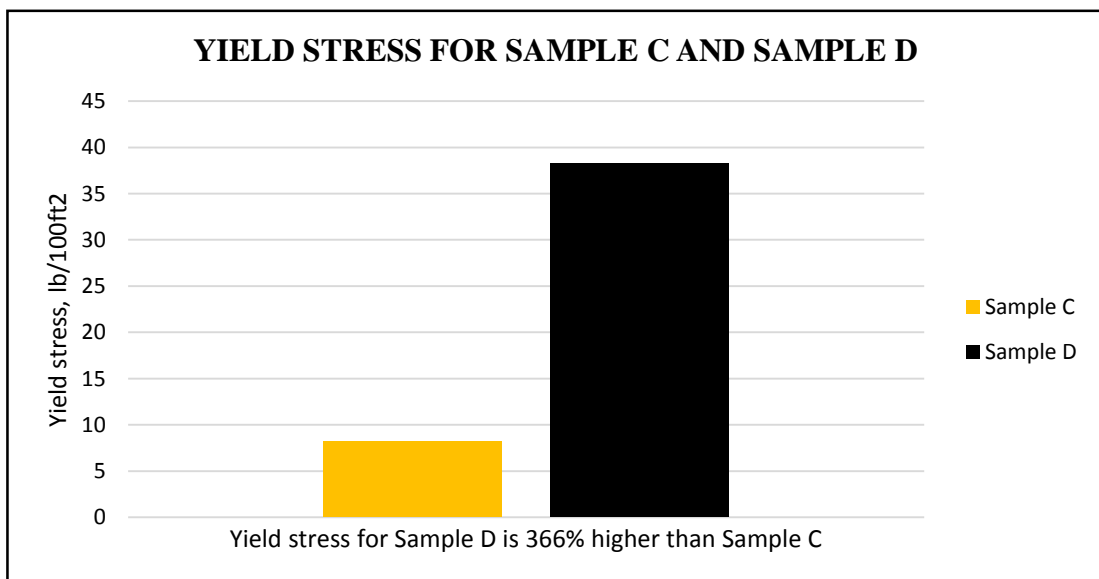


Figure 52. Yield Stress for Sample C and Sample D

Plastic viscosity is defined as an indication of the number, size and shape of solids in a fluid while the yield point measure the attraction that occurs between solids in the fluid itself [48].

Figure 51 and Figure 52 increase in the percentage of micro silica from 40% to 60% show significant increase in PV and YP of the cement samples.

For the same weight, particle with smaller size and less weight will have high solid contents. Micro silica has smallest size and lowest weight compares to fly ash and Class G Cement [46]. As defined, plastic viscosity is a function of solid content, thus increase in micro silica will increase the solid content and resulted in high plastic viscosity.

High yield stress in Sample D compared to Sample C is caused by binding of large amounts of water by micro silica, thus hinder the water from lubricating the flow of larger grain and require additional stress to initiate the flow [45].

4.4 DENSITY TEST

Density test for all samples are done using pressurized mud balance standard condition and the result are as in the Figure 53.

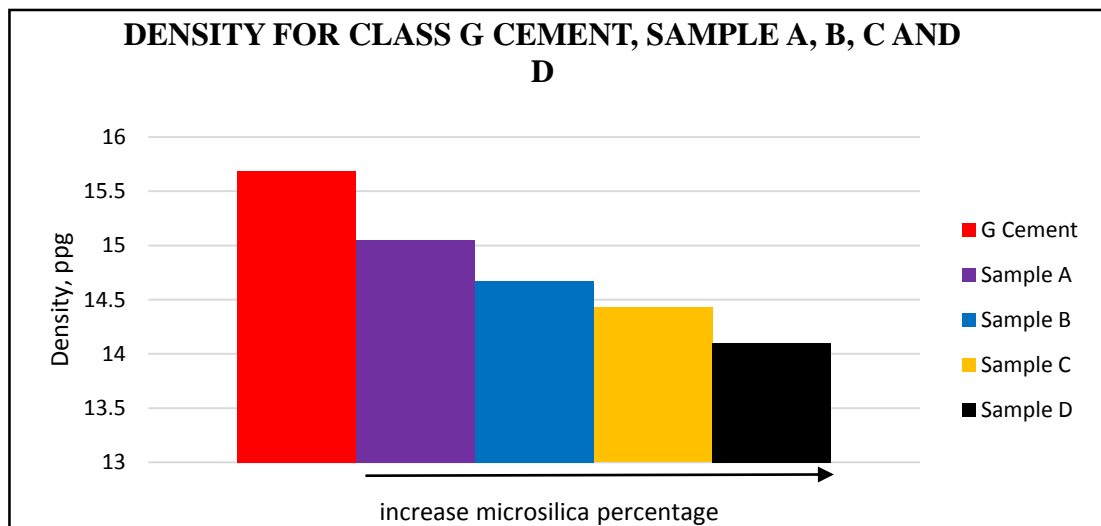


Figure 53. Graph of density for Class G Cement, Sample A, B, C and D

Table 10. Density for Class G Cement, Sample A, B, C and D.

Weight of Materials, g	Specific gravity	Percentage difference with Class G Cement				
		Cement G	Sample A	Sample B	Sample C	Sample D
Ordinary Portland Cement	3.15	0%	4.08%	6.5%	8.03%	10.13%
Class F Fly Ash	2.38					
Micro silica	2.22					

Figure 53 shows the reduction in density of cement samples as the percentage of micro silica increase and percentage of class F fly ash decrease. Cement G has the highest density while Samples D consist of 40% of fly ash and 60% of micro silica shows the lowest density with 10.13% density difference compared to Class G Cement.

Density differences for each samples are affected by difference in specific gravity of each material in the mixture formulations. Materials with high specific gravity resulted in high density cement samples. According to Figure 53. Graph of density for Class G Cement, Sample A, B, C and D

Table 10 show micro silica has the lowest specific gravity followed by fly ash and Class G Cement and therefore Sample D which contain highest percentage of micro silica has the lowest density.

CHAPTER 5

CONCLUSSIONS AND RECOMMENDATIONS

5.1 CONCLUSIONS

From the obtained data, it can be concluded that:

1. Sample A, B and C which contain (0%, 20% and 40% of micro silica) can replaced Ordinary Portland Cement in high pressure high temperature well (4000psi and 120°C).
2. Sample D which consists of 60% of micro silica cannot replaces Ordinary Portland Cement in HPHT well due to degradation of micro silica.
3. High curing temperature will cause the micro silica to degrade, thus increase the permeability of the cement samples.
4. Increase in curing duration will increase the permeability of cement due to weakening of microstructure.
5. Micro silica and fly ash have significant effect in improvinClass G Cement fluid loss at low pressure low temperature condition (500psi and 70°C). All geopolymer cement samples have less than 10ml/30 min of volume of filtrate.
6. Micro silica has significant effect in increasing the viscosity of cement sample due to high specific surface area, but the viscosity of Sample A and Sample B are still below the viscosity of Class G Cement. High specific surface area of micro silica tends to absorb more water compare to small specific surface area material.
7. Micro silica can reduce the density of cement sample due to low specific gravity compare to fly ash and Class G Cement.

5.2 RECOMMENDATIONS

Suggested further works for expansion and continuation:

1. Vary the curing temperature from 20° C to 200° C to observe the effect of temperature on cement performance.
2. Increase the curing duration to one month to observe the permeability of cement in down hole condition against time.
3. Replace micro silica with nano silica and compare the performance of both against temperature.

REFERENCES

- [1] Smith, D. K. (1897). *Cementing*. United States of America: Society of Petroleum Engineers.
- [2] Schneider, M., Romer, M., M.Tschudin, & Bolio, H. (2011). Sustainable cement production - present and future. *Cement and Concrete Research*, 642-650.
- [3] Nasvi, M., & Ranjith, P. S. (2012). Comparison of mechanical behaviors of geopolymers and Class G Cement as well cement at different curing temperatures for geological sequestration of carbon dioxide. *ARMA* 12-232.
- [4] CEMENT TEST EQUIPMENT. (2014). Retrieved from <http://www.ctetulsa.com/>
- [5] Mohamed, C. N., Ranjith, P., & Sanjayan, J. (2012). Mechanical Properties of geopolymer cement in brine: its suitability as well cement for geological sequestration of carbon dioxide. *7th Asian Rock Mechanics Symposium*, (pp. 1034-1040). Seoul.
- [6] Teodoriu, C., Amani, M., Yuan, Z., Schubert, J., & Kosinowski, C. (2012). Investigation of the Mechanical Properties of Class G Cement and Their Effect on Well Integrity. *International Journal of Engineering and Applied Sciences*.
- [7] Bignozzi, M. C. (2011). Sustainable cement for green buildings construction. *2011 International Conference on Green Buildings and Sustainable Cities* (pp. 915-921). Elsevier Ltd.
- [8] Hasanbeigi, A., Price, L., & Lin, E. (2012). Emerging energy-efficiency and CO₂ emission-reduction technologies for cement and concrete production : A technical review. *Renewable and Sustainable Energy Reviews*, 6220-6238.
- [9] Imbabi, M. S., Carrigan, C., & McKenna, S. (2012). Trends and development in green cement and concrete technology. *International Journal of Sustainable Built Environment*, 194-216.
- [10] Jannie, S. V., John, L. P., & Duxson, P. (2012). Technical and commercial progress in the adoption of geopolymer cement. *Mineral Engineering*, 89-104.
- [11] Mixhaux, M., Nelson, E., & Vidick, B. (n.d.). *Cement Chemistry and Additives*. In *OILFIELD REVIEW* (pp. 18-25). France.
- [12] Salehi, R., & Paiaman, A. M. (2009). A Novel Cement Slurry Design Applicable to Horizontal Well Conditions. *Petroleum & Coal*, 270-276.
- [13] Raki, L., Beaudoin, J., Alizadeh, R., Makar, J., & Sato, T. (2010). Cement and Concrete Nanoscience and Nanotechnology. *Materials*, 918-942.
- [14] Patil, R., & Deshpande, A. (2012). Use of Nanomaterials in Cementing Application. *Society of Petroleum Engineers*.
- [15] Etal, G. M. (1957). *Well Completion With Permeable Concrete*.
- [16] Murtaza, M., Rahman, M., Al-Majed, A., & A.Samad. (2013). Mechanical, Rheological and Microstructural Properties of Saudi Type Class G Cement Slurry with Silica Flour Used in Saudi Oil Field under HPHT Conditions. *Society of Petroleum Engineers*.

- [17] Ozyurtkan, M. H., Gursat Altun, I. M., & Serpen, U. (2013). An Experimental Study on Mitigation of Oil Well Cement Gas Permeability. International Petroleum Technology Conference.
- [18] Iverson, B., Maxson, J., & Bour, D. (2010). Strength Retrogression in Cements Under High Temperature Conditions. Thirty-Fifth Workshop on Geothermal Reservoir Engineering. California.
- [19] Ostroot, G. W., Aime, M., & Walker, W. A. (1961). Improved Compositions for Cementing Wells with Extreme Temperatures. Society of Petroleum Engineers, 277-284.
- [20] Teodoriu, C., Kosinowski, C., Amani, M., Schubert, J., & Shadravan, A. (2012). Wellbore Integrity and Cement Failure at HPHT Conditions. International Journal of Engineering and Applied Sciences.
- [21] Nikiforuk, A. (2013, January 9). Shale Gas: How Often Do Fracked Wells Leak? Retrieved from THE TYEE: <http://theyee.ca/News/2013/01/09/Leaky-Fracked-Wells/>
- [22] Kamhangrittirong, P. (2008). THE EFFECT OF ALKALI SOLUTION RATIO AND CURING TEMPERATURE ON PROPERTIES OF FLY ASH BASED GEOPOLYMER. OUR WORLD IN CONCRETE & STRUCTURES. Singapore: Singapore Concrete Institute.
- [23] Bakri, A. M., H.Kamarudin, M.Bnhussain, Nizar, I., Rafiza, A., & Y.Zarina. (2011). Microstructure of different NaOH molarity of fly ash-based green polymeric cement. Journal of Engineering and Technology Research Vol 3(2), 44-49.
- [24] Bakri, A. A., Kamarudin, H., Bnhussain, M., Nizar, I. K., A.R.Rafiza, & Y.Zarina. (2011). THE PROCESSING, CHARACTERIZATION, AND PROPERTIES OF FLY ASH BASED GEOPOLYMER CONCRETE.
- [25] What are Coal Combustion By-Product (CCBs)? (2014, 1 14). Retrieved from University of Kentucky Center for Applied Energy Research: <http://www.caer.uky.edu/kyasheducation/flyash.shtml>
- [26] Abbas, G., Irawan, S., Kumar, S., & Elrayah, A. A. (2013). Improving Oil Well Cement Slurry Performance Using Hydroxypropylmethylcellulose Polymer. Advanced Materials Research Vol. 787, 222-227.
- [27] Black, J. R. (n.d.). Mix Design Process for Alkaline-Activated Class F Fly Ash Geopolymer Concrete.
- [28] Shahrudin, S., Samsuri, A., Suhaimi, A., Nasir, A. S., & Ahmad, Z. (n.d.). Possibility Studies Of Using Local Cement In Oil And Gas Wells Cementing Operations In Malaysia.
- [29] Neville, A., & Brooks, J. (2010). CONCRETE TECHNOLOGY. England: Pearson Education Limited.
- [30] Scientific Principles. (n.d.). Retrieved from Materials Science and Technology: <http://matse1.matse.illinois.edu/concrete/prin.html>
- [31] Davidovits, J., Davidovits, R., & Davidovits, M. (2012). Geopolymeric Cement Based On Fly Ash and Harmless to Use.

- [32] Xian, T. H. (n.d.). Geopolymer based Oil Well Cementing Systems using Micro silica.
- [33] P.Eswaramoorthi, & Arunkumar, G. (2014). Fibers Study On Properties Of Geopolymerconcrete With Polypropylene. *International Refereed Journal of Engineering and Science (IRJES)*, 60-75.
- [34] INSTITUTE, A. P. (2002). Specification for Cements and Materials for Well Cementing. AMERICAN PETROLEUM INSTITUTE.
- [35] INSTITUTE, A. P. (2010). Recommended Practice for Testing Well Cements. AMERICAN PETROLEUM INSTITUTE.
- [36] Unsteady state gas permeameter and porosimeter - Coreval 30. (2014). Retrieved from VINCI TECHNOLOGIES Laboratory and field instruments for Petroleum Industry:<http://www.vinci-technologies.com/products-explo.aspx?IDM=753566&IDR=82292&IDR2=82525>
- [37] The Geopolymer Solution. (2012). Retrieved from THE Zeobond GROUP: <http://www.zeobond.com/geopolymer-solution.html>
- [38] Shadizadeh, S., M.Kholghi, & Kassaei, M. S. (2010). Experimental Investigation of Micro silica as a Cement Extender for Liner Cementing in Iranian Oil/Gas Wells. *Iranian Journal of Chemical Engineering*, 42-66.
- [39] Memon, K. R., Shuker, M. T., Tunio, S. Q., Lashari, A. A., & Abbass, G. (2013). Investigating Rheological Properties of High Performance Cement System for Oil Wells . *Research Journal of Applied Sciences, Engineering and Technology* 6, 3865-3870.
- [40] Eilers, L., Nelson, E., & Moran, L. (1983). High-Temperature Cement Compositions- Pectolite, Scawtite, Truscottite or Xonotlite: Which Do You Want? *JOURNAL OF PETROLEUM TECHNOLOGY*, 1373-1377.
- [41] Khater, H. M. (2013). Effect of micro silica on the characterization of the geopolymer materials. *International Journal of Advanced Structural Engineering* .
- [42] Mueller, D., & III, R. D. (1991). The Versatility of Micro silica as an Oilwell Cement Admixture. *Production Operations Symposium*. Oklahoma: Society of Petroleum Engineers.
- [43] Rheology of Drilling Mud. (2014). Retrieved from <http://rishibabuadari.tripod.com/MudRheology/Rheology.htm>
- [44] Adriano Papo, L. P. (2010). Rheological Properties of Very High-Strength Portland Cement Pastes: Influence of Very Effective Superplasticizers. *International Journal of Chemical Engineering*.
- [45] Rune Godoy, A. S. (2004). Experimental Analysis of Yield Stress in High Solids Concentration Sand Slurries used in Temporary Well Abandonment Operations. *ANNUAL TRANSACTIONS OF THE NORDIC RHEOLOGY SOCIETY*, 81-84.
- [46] Helge Hodne, A. S. (2001). Rheological Properties of High Temperautre Oil Well Cement Slurries . *ANNUAL TRANSACTIONS OF THE NORDIC RHEOLOGY SOCIETY*.

- [47] Physical Properties and Chemical Composition of Microsilica. (2011, 5 29). Retrieved from China Microsilica Union: <http://www.chinamicrosilica.com/tech/113.html>
- [48] Wcdrake. (2014). NewPark Mud Report Study. Retrieved from Quizlet: <http://quizlet.com/5817514/newpark-mud-report-study-flash-cards/>
- [49] Art Bonett, D. P. (1996). Getting to the Root of Gas Migration. *Oilfield Review*, 36-49.
- [49] *Micro silica*. (2014, 7 2). Retrieved from WIKIPEDIA: http://en.wikipedia.org/wiki/Silica_fume
- [51] THE EFFECT OF MICRO SILICA ON THE PROPERTIES OF CONCRETE AS DEFINED IN CONCRETE SOCIETY REPORT 74, CEMENTITIOUS MATERIALS. (29-31 August 2012). OUR WOLRD IN CONCRETE & STRUCTURES. Singapore: Singapore Concrete Institute.
- [52] Nediljka Gaurina-Medimurec, D. M. (1994). CEMENT SLURRIES FOR GEOTHERMAL WELLS CEMENTING. *Rudarsko-geoloSko-naftni zbornik*, 127-134.
- [53] Jallo, E. K. (2012). Experimental Study on the Behaviour of High Strenght Concrete with Micro silica under Monotonic and Repeated Compressive Loads. *Al-Rafidain Engineering*, 55-65.
- [54] Micro silica And Its Effects On Concrete Properties Health Essay. (2014). Retrieved from UKESSAYS.com: <http://www.ukessays.com/essays/health/silica-fume-and-its-effects-on-concrete-properties-health-essay.php#ixzz36Ee1s4Ue>
- [55] Dillenbeck, L. (2010). The Impact of Cementing On Proper Well Control. Retrieved from http://www.iadc.org/wp-content/uploads/The-impact-of-well_-cementing-on-proper-well-control.pdf
- [56] M.C.M. Nasvi, P. R. (2014). Effect of temperature on permeability of geopolymer: A primary well sealant for carbon capture and storage wells. *Fuel*, 354-363.
- [57] Services. (n.d.). Retrieved from Powerflex Services, Inc. : <http://www.powerflexcementers.com/services>
- [58] Fluid Loss Test Instrument Single Cell Instruction Manual. (2014, 05). Retrieved from Fann Instrument Company: http://www.fann.com/public1/pubsdata/Manuals/Single_Cell_Static_Fluid_Lost_Test.pd
- [59] Nanyang City Srate Optical Instrument Manufactory. (2014). Retrieved from globalsources: <http://srate.manufacturer.globalsources.com/si/6008836201676/pdtl/PCB-processing/1084678691/PCB-Inspection-Microscope.htm>